Dynamic Analysis and Structural Optimization of a Fiber Optic Sensor Using Neural Networks

Yong-Yook Kim
The Center for Healthcare Technology Development, Chonbuk National University, Duckjin-dong, Jeonju, Jeonbuk 561-756, Korea
Rakesh K. Kapania, Eric R. Johnson
Department of Aerospace and Ocean Engineering, Virginia Polytechnic Institute and State University, Blacksburg, VA 24061, USA
Matthew E. Palmer
Luna Innovations Inc., 2851 Commerce St SE, Blacksburg, VA 24060, USA
Tae-Kyu Kwon*, Chul-Un Hong, Nam-Gyun Kim
Division of Bionics and Bioinformatics, Chonbuk National University, Duckjin-dong, Jeonju, Jeonbuk 561-756, Korea

The objective of this work is to apply artificial neural networks for solving inverse problems in the structural optimization of a fiber optic pressure sensor. For the sensor under investigation to achieve a desired accuracy, the change in the distance between the tips of the two fibers due to the applied pressure should not interfere with the phase change due to the change in the density of the air between the two fibers. Therefore, accurate dynamic analysis and structural optimization of the sensor is essential to ensure the accuracy of the measurements provided by the sensor. To this end, a normal mode analysis and a transient response analysis of the sensor were performed by combining commercial finite element analysis package, MSC/NASTRAN, and MATLAB. Furthermore, a parametric study on the design of the sensor was performed to minimize the size of the sensor while fulfilling a number of constraints. In performing the parametric study, the need for a relationship between the design parameters and the response of the sensor was fulfilled by using a neural network. The whole process of the dynamic analysis using commercial finite element analysis package and the parameter optimization of the sensor were automated within the MATLAB environment.

Key Words : Structural Optimization, Artificial Neural Network, Fiber Optic Pressure Sensor, Mode Superposition Method, Mode Acceleration Method

1. Introduction

Optical fiber sensors have advantages over conventional sensor in many aspects such as higher spatial and temporal resolution, the immunity to electromagnetic interference, lightweight, small size, easy multiplex capability, and large bandwidth. Due to their superior qualities in many aspects, they have many applicable areas including strain measurements, pressure measurements, structural health monitoring, rotation sensing, chemical/biomedical sensors, and etc. The general use and the development of fiber optic sensors have been reviewed by Kersey (1996). The use of fiber optic sensors in electrical field has been recently reviewed by Lee (2003). The feasibility

* Corresponding Author,
E-mail : kwon10@chonbuk.ac.kr
TEL : +82-63-270-4066; **FAX** : +82-63-270-2247
Division of Bionics and Bioinformatics, Chonbuk National University, Duckjin-dong, Jeonju, Jeonbuk 561-756, Korea. (Manuscript **Received** June 28, 2005; **Revised** December 20, 2005)

of using fiber optic sensors for biosensor has been investigated by number of researchers (Yang et al., 2003; Kaufman et al., 2003). Yang et al. proved the biocompatibility of a fiber optic micro pressure sensor which can be used for in-vivo human application. Successful applications of fiber optic sensors toward structural health monitoring have been reported by number of researchers as well (Li et al., 2004; Leung et al., 2005). There also has been a unique application of fiber optic pressure sensor toward a biomedical device such as the construction of a smart bed (Spillman et al., 2004; Li et al., 2004).

The capability of NNs has been utilized in various design optimization problems by many researchers. Mukherjee and Deshpande (1995) combined NNs with rule-based expert system (RBES) approaches to overcome the shortcomings of RBES; Namely, that the RBES lacks a learning capability and that the rules need to be stated explicitly. They used a mathematical optimization model to generate the training set and the testing set for NNs. Jayatheertha et al.(1996) applied a simulated annealing process in their approach in optimizing the configuration of a laminated composite plate. Simulated annealing is a statistical training method and resembles the annealing of a metal. Park et al.(2003) used a neural network to predict life cycle assessment. Kim et al.(2004) used a neural network in ship hull plate classification to predict cost for a preliminary ship design. Cho et al.(2004) used a neural network to improve both maneuverability and durability of tire. They used a back-propagation neural network model for faster approximations of the objective functions using finite difference scheme. Lee et al.(2004) used a neural network in the design process of stereolithography.

Ramasamy et al.(1996) used a feed-forward backpropagation neural network in an expert system and compared the optimization results with those of the genetic algorithm in designing a truss roof system. Rai et al.(2000) started the design process with the initial condition from the reference design and used a sequence of response surfaces based on both neural networks and polynomial fits in traversing the design space to find an optimal dimension of an airfoil.

Nikolaidis et al.(2000) used NNs and response surface polynomials to rapidly predict the performance characteristics of an automotive joint given the component dimensions. They found that the performance of NNs and the response surface polynomials are very similar to each other. Kaveh et al.(2001) used feed-forward backpropagation NNs to predict the maximum deflection and the weight in the design of double layer grids for minimum weight. They used a data ordering method to reduce the nonlinearity of the data and to increase the speed of the training.

Greenman et al.(2002) combined a bootstrap technique that estimates network generalization performance with stochastic and deterministic optimization techniques in adjusting the interconnection geometry of NNs to optimize a NN that models a multi-element airfoil with small training data sets. Hadi (2003) used NNs in optimizing a concrete beam for weight and cost with strength and serviceability constraints by storing many optimum designs and training a neural network for the stored design. They also used this approach in optimizing the design of fiber reinforced concrete beams. Ha et al.(2004) used a neural network to model uncertain factors.

The most important features that were utilized from NNs in most design processes listed above were the NNs' superior generalization quality that is capable of extracting significant information from a massive set of data, and the ability to cope with the ill-defined problems. One of the main problems in applying NNs for engineering optimization problems is that the process of obtaining the solution for different design parameters is done manually and preparing the data to train NNs' takes a great amount of CPU time. In this work, this problem has been solved by automating the whole optimization process including solving the direct and inverse problems.

In constructing response surface for the optimization process, the most commonly used neural network structure, the multi-layer feed-forward backpropagation neural network as shown in Fig. 1 was used. The hidden neurons are trans-

ferred sums of weighted inputs p with added bias, and the outputs t of the network are transferred sums of weighted hidden neuron values a with added bias. A sigmoid function was used in hidden layers and a linear function was used in the output layer in our case. The relationship between input and output of a NN is shown in Eq. (1).

$$a_i = f\left(\sum_{j=1}^{r} w_{ij}^1 \cdot p_i + b_i^1\right)$$
$$t_i = \bar{f}\left(\sum_{j=1}^{s} w_{i,j}^2 \cdot a_i + b_i^2\right) \quad (1)$$

where w is weight and f is a transfer function (Haykin 1998, Hagan et al., 1996).

The subject of this paper is a miniature fiber optic pressure sensor, being manufactured by Luna Innovations Inc, Blacksburg, VA, USA and made of a silicon base and two optical fibers mounted in V-grooves of the base. See Fig. 2. When the air pressure between the two fibers is changed, the density of the air is changed and this change results in a phase change of the light passing through the fiber that is reflected from the surface of the gap between the two fibers. For the sensor to be able to achieve a desired accuracy, the change in the distance between the two fibers due to the pressure change should not interfere with the phase change due to the change in the density of the air between the two fibers. Therefore, accurate dynamic analysis of the sensor is essential to ensure the accuracy of the measurement made by the sensor

Here, the normal mode analysis and the transient response analysis of the sensor were performed using commercially available packages, MSC/PATRAN and MSC/NASTRAN. Furthermore, a parametric study on the design of the sensor was performed to minimize the size of the sensor while fulfilling a number of constraints. In performing the parametric study, the need for a relationship between the design parameters and the response of the sensor was achieved by using artificial neural network (NN) instead of calculating the response of the sensor for all the possible variation of the parameters. A feed-forward back-propagation NN was trained to map the relation between the design parameters and the response of the sensor. The gradient-based optimization method of MATLAB was used to perform the optimization using NN.

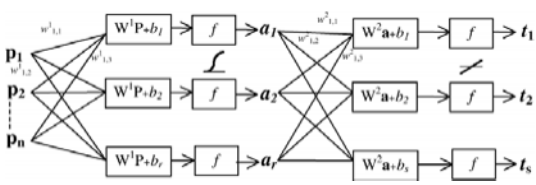

Fig. 1 Multil-layer feed-forward backpropagation neural network with a sigmoid transfer function for the hidden layer and linear transfer funciton for the output layer. (p=inputs, a=hidden neurons, w=weights, b=bias, f=transfer function, n=number of inputs, r=number of hidden neurons, s=number of output neurons, t=outputs)

2. Finite Element Modeling of the Sensor

The miniature fiber-optic sensor analyzed here is a sensor which is used to accurately measure the

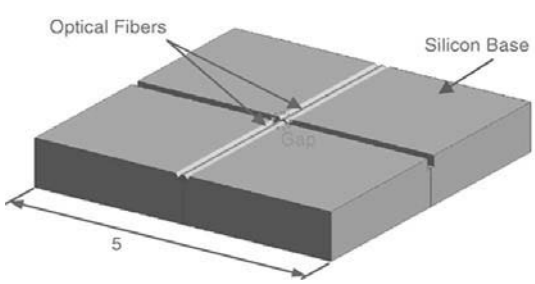

(a) Fiber optic pressure sensor

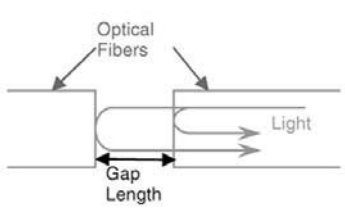

(b) Light paths near the gap area

Fig. 2 Geometric drawing of the miniature fiber- optic pressure sensor and the light paths around the gap area

pressure change in the air by utilizing the phase change in the optical fiber used in the fiber optic sensor. Figure 2(a) shows the geometric drawing of the sensor and Fig. 2(b) shows the detailed drawing around the gap area of the sensor displaying two light paths in the optical fiber that reflects from two surfaces. The change in the phase difference between two light paths occurs as a result of the change in the air density in the gap area due to pressure changes in the air surrounding the fiber. This change is measured to accurately determine the pressure change. However, the structural vibration can also result in a change in the phase difference. Therefore, structural analysis and design optimization is essential to minimize the interference between the structural vibration of the sensor and air density changes.

A three-dimensional finite element model was used to analyze and optimize the miniature fiber optic sensor. This model represents one quarter of the sensor that represents the whole model by employing two planes of symmetry. Figure 3 shows the full finite element model and one quarter of the finite element model. The quarter model is represented using a hexagonal finite element that has 20 nodes. The model has 4,593 nodes and 838 elements, and has 13,677 degrees of freedom. In the quarter model, the boundary conditions at the bottom only allow sliding displacements on the bottom plane and the boundary conditions at the side that faces symmetric half only allow sliding displacements on the plane of the side.

2.1 Normal mode analysis

A modal analysis was performed to obtain the natural frequencies and the modal displacement vector of the sensor. The calculation was done using the MSC/NASTRAN normal mode solver. In studying the normal modes of the sensor, two kinds of boundary conditions were considered. One was a sliding bottom boundary condition and the other was a fixed bottom boundary condition.

The mode shapes for each case were also studied to find the modes that can affect the displacements of the fiber at the gap. For the sliding boundary condition, the 3rd mode and the 7th mode were found to have the most influence on the displacement at the gap area. Figure 4 shows

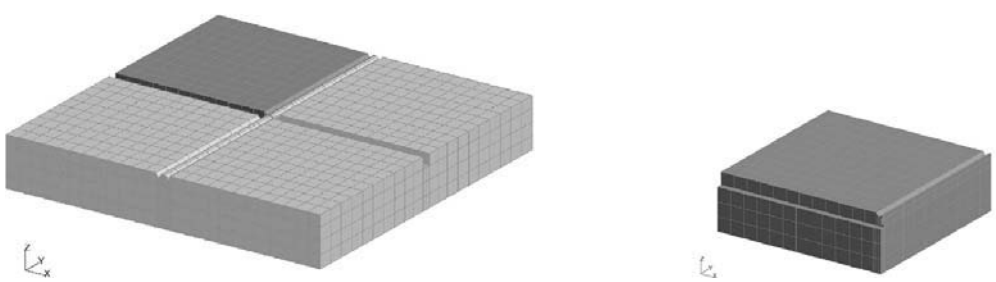

(a) The FEM model for the whole sensor (b) The quarter model

Fig. 3 Finite Element Model of the miniature fiber- optic sensor

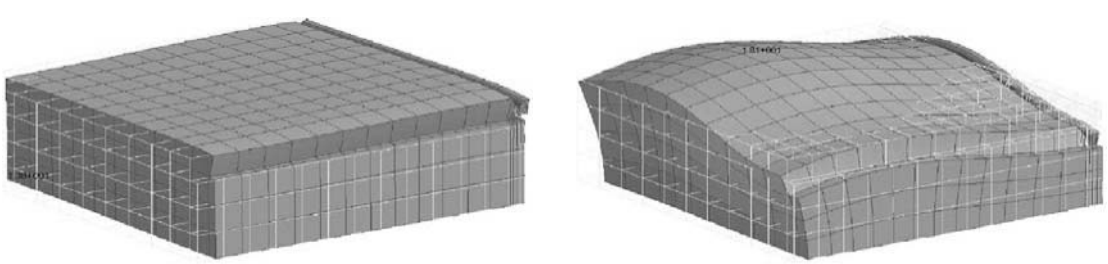

(a) 3rd mode (b) 7th mode

Fig. 4 The mode shapes of the sensor with sliding bottom boundary condition

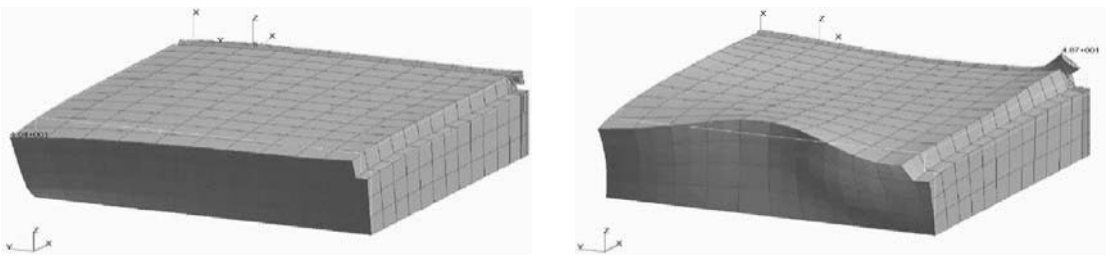

(a) 2nd mode (b) 8th mode

Fig. 5 The mode shapes of the sensor with fixed bottom boundary condition

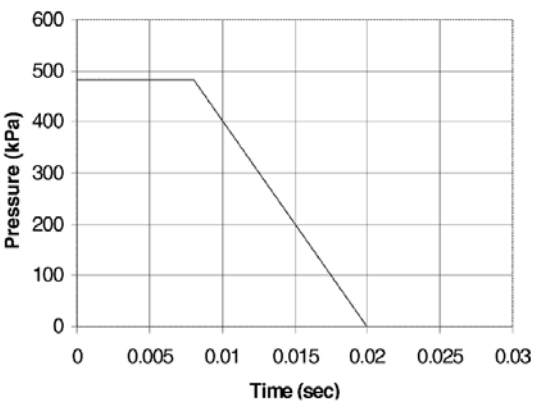

Fig. 6 Pressure Time-history approximated from experimental data

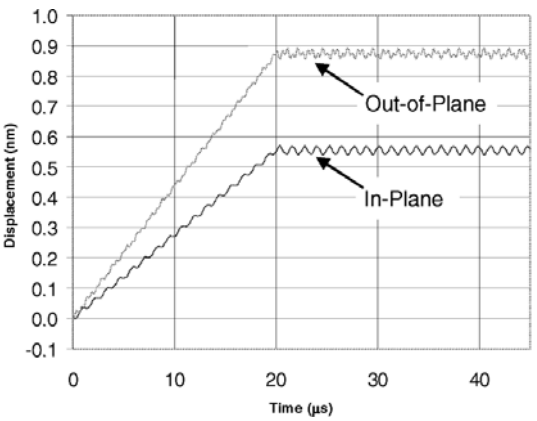

Fig. 7 Calculated time history of the displacements at the tip of the fiber, obtained using NASTRAN

these two modes. For the fixed bottom condition, the 2nd and the 8th modes were found to be most influential on the response of the sensor, as shown in Fig. 5.

2.2 Transient response analysis using direct method

A transient response analysis was performed using a transient input that was obtained from an experiment. The approximate experimental pressure profile used here consists of a pressure rise to 70 psi in 20 microseconds, and the trailing edge is approximated by a line from $t=0.008$ sec and $p=$ 70 psi to $t=0.02$ sec and $p=0$ psi. This pressure profile is shown in Fig. 6.

The transient response was calculated using NASTRAN's direct time-integration method with a sliding bottom boundary condition. Figure 7 shows the time history of the displacement of the gap. The analysis was performed only for a short duration of time that includes the pressure rise

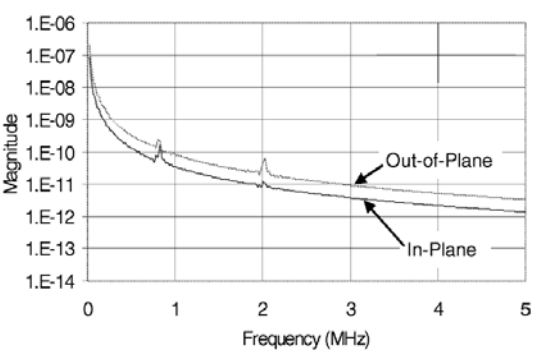

Fig. 8 FFT of the response at the tip of the sensor

because of the available computational resources.

The Fast Fourier Transform (FFT) of the time history of the gap displacement was obtained. See Fig. 8. The small peaks are at 0.808 MHz and 2.13 MHz which correspond to the 3rd and 7th modes, respectively.

A functional form of a pressure profile shown

in Fig. 9 and given by

$$p(t) = p_0 - p_s^- \left(\frac{t}{T^-}\right)\left(1 - \frac{t}{T^-}\right) e^{-4\frac{t}{T^-}} \qquad (2)$$

where t denotes time, p_0 ambient pressure, p_s^- peak negative phase, and T^- the duration of the negative pressure phase (Baker 1973) was used as the pressure profile in most of the cases in this research, because this includes both the positive and negative phases of the pressure profile.

The modal analysis capability in NASTRAN was used to approximate the transient response. For the fixed bottom boundary condition, we retained fifty modes. The time step for integrating the modal equations was selected to be one-tenth of the time for a wave to traverse the thickness of the base. We compared the modal method to the direct method of integration. Figure 10 shows the time history of the change in the gap size obtained using a direct time integration scheme.

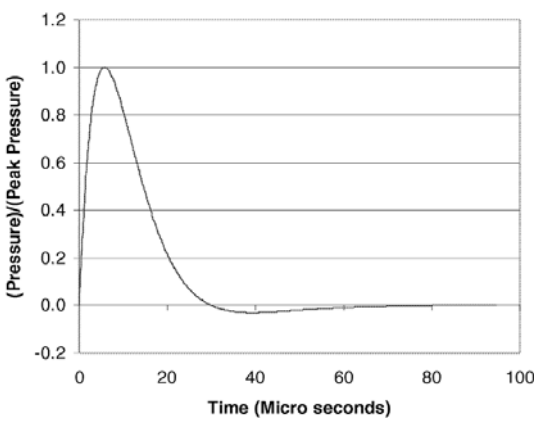

Fig. 9 Time history of the pressure profile including the phase in which pressure turns into suction

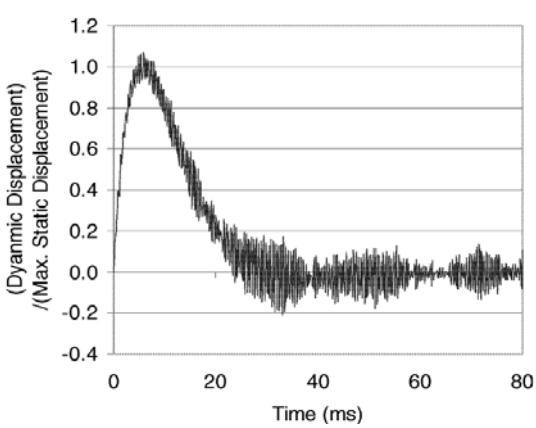

Fig. 10 Time history of the gap change obtained with NASTRAN's direct method

Next, an FFT analysis was performed on the time history of the gap displacement of the sensor. Figure 11 shows the FFT of the output divided by the FFT of the input. Here, the highest peak for the modal case was found to be at the 2nd and the 8th modes. In Figure 11, we can find that the results from the direct method correspond to the high peaks of the modal method results.

The transient response calculation using the direct method in NASTRAN took a relatively long period of time, and required a large amount of disk space. In the current case, which uses the three-dimensional FEM model and 1000 time steps, the calculation took about one-half hour and required about 1GB of disk space. Therefore, we needed to have a method that could speed up the calculation and require much less disk space to perform a parametric study, because a parametric study requires repeated calculations of the transient response for different design parameters. The modal methods explained in the next section, was employed to overcome this problem of excessive CPU time and storage requirements.

2.3 Transient response analysis using modal methods

Any forced motion of a linear Multi-Degree-Of-Freedom (MDOF) system may be expressed in terms of forced modal vibrations. We first used

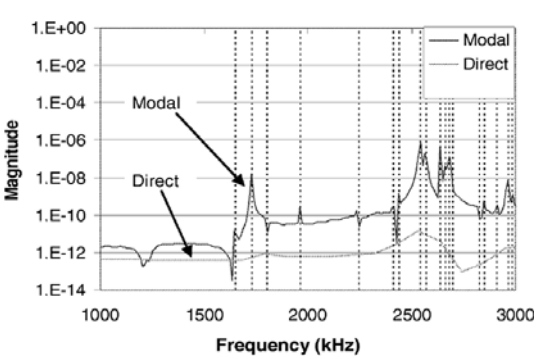

Fig. 11 FFT of Output divided by FFT of Input using the Modal superposition method

the classic modal superposition method. The dynamic equation for a case of Multi-Degree-of-Freedom (MDOF) systems can be expressed as

$$\mathbf{M}\ddot{\mathbf{u}}+\mathbf{K}\mathbf{u}=\mathbf{p}(t) \tag{3}$$

where $\mathbf{M}$ is the mass matrix, $\mathbf{K}$ is the stiffness matrix, $\mathbf{u}$ is the displacement vector, and $\mathbf{p}$ is the forced input. Here, the effect of damping of the structure was not considered.

The first step in a modal superposition method is to obtain natural frequencies and normal modes of the system. The natural frequencies and modes satisfy

$$(\mathbf{K}-\omega_r^2\mathbf{M})\,\phi_r=\mathbf{0} \tag{4}$$

The modes can be collected to form the so-called modal matrix

$$\Phi=[\phi_1\ \phi_2\ \cdots\ \phi_N] \tag{5}$$

The coordinate transformation that relates the displacement vector and the modal displacement vector is

$$\mathbf{u}(t)=\Phi\eta(t)=\sum_{r=1}^{N}\phi_r\eta_r(t) \tag{6}$$

The reduced dynamic equation can be expressed in terms of the modal displacement vector as

$$\bar{\mathbf{M}}\ddot{\boldsymbol{\eta}}+\bar{\mathbf{K}}\boldsymbol{\eta}=\bar{\mathbf{p}}(t) \tag{7}$$

where the modal mass matrix is calculated as $\bar{\mathbf{M}}=\Phi^t\mathbf{M}\Phi$, the modal stiffness matrix $\bar{\mathbf{K}}=\Phi^t\mathbf{K}\Phi$, and the modal force vector $\bar{\mathbf{p}}=\Phi^t\mathbf{p}$. The components of the modal displacement vector $\boldsymbol{\eta}$ can be obtained by solving the equations independently since the modal mass and stiffness matrices have diagonal form.

The modal acceleration method can account for the effects of higher modes in the modal analysis with a small number of modes (Craig 1981). Therefore, the modal acceleration method has many advantages over the modal superposition method including the improved convergence properties and more accurate results with a smaller number of modes. The dynamic equation for MDOF system shown in Eq. (3) can be expressed as:

$$\mathbf{u}=\mathbf{K}^{-1}(\mathbf{p}-\mathbf{M}\ddot{\mathbf{u}}) \tag{8}$$

$$\mathbf{u}=\mathbf{K}^{-1}\mathbf{p}-\mathbf{K}^{-1}\sum_{r=1}^{N}\mathbf{M}\Phi_r\ddot{\boldsymbol{\eta}}_r \tag{9}$$

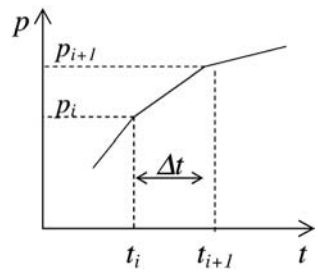

Fig. 12 Piecewise linear approximation of the forced input. This allows us to use exact integration between t_i and t_{i+1}

The solution of Eq. (9) can be obtained by solving for the modal acceleration vector $\ddot{\boldsymbol{\eta}}$ from Eq. (7).

A piecewise linear approximation of applied force, as shown in Fig. 12, was utilized in solving the independent equations (7). The exact solution of the equation below was used in piecewise fashion to obtain $\boldsymbol{\eta}$ and $\ddot{\boldsymbol{\eta}}$.

$$\begin{aligned}\bar{\mathbf{M}}\ddot{\boldsymbol{\eta}}+\bar{\mathbf{K}}\boldsymbol{\eta}&=at+b,\ t_i<t<t_{i+1}\\ \boldsymbol{\eta}(t_i)&=\boldsymbol{\eta}_i\\ \dot{\boldsymbol{\eta}}(t_i)&=\dot{\boldsymbol{\eta}}_i\end{aligned} \tag{10}$$

The use of the modal method to approximate the transient response permitted a much larger number of time steps within the available computational resources. The transient response was calculated using the modal superposition method in MATLAB based on normal modes extracted from NASTRAN. The results of the modal superposition method were close to those of the NASTRAN modal method when the same numbers of modes were used as can be seen in Fig 13(a). As the number of modes increased, the results from modal superposition were close to those of NASTRAN's direct method as shown in Fig. 13(b).

Next, the transient response was calculated using the modal acceleration method. As can be seen in Fig. 14, the results of the modal acceleration method were close to those of the NASTRAN direct method even when a small number of modes were used.

The advantage of the modal acceleration method is that it saves considerable CPU time compared to the CPU time required by the direct method used in NASTRAN. Table 1 shows the

Table 1 The comparison of CPU time for calculating the transient response with different methods

Method	NASTRAN Direct	NASTRAN Modal (50 modes)	Mode Superposition (50 modes)	Mode Acceleration (10 modes)
Time	6 m 20 s	1 m 02 s	39 sec	10 sec
Relative	38	6	4	1

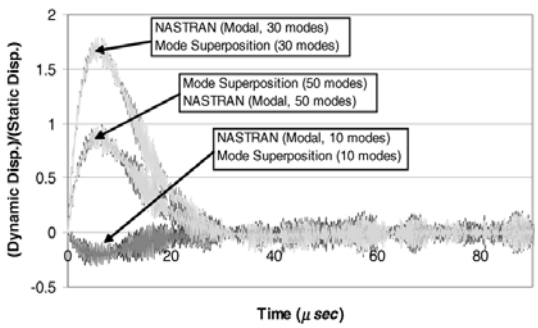

(a) Comparison of Mode superposition method solutions using MATLAB with NASTRAN modal solution

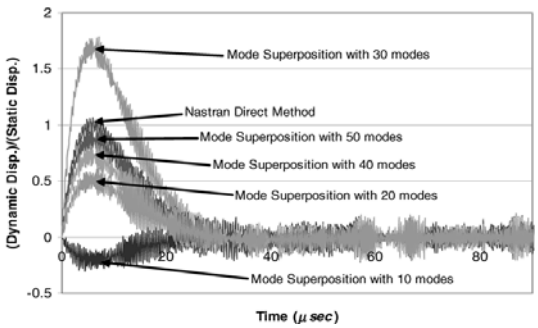

(b) Comparison of Mode superposition method solutions using MATLAB with NASTRAN direct method solution

Fig. 13 Time history of the gap displacement using modal superposition method

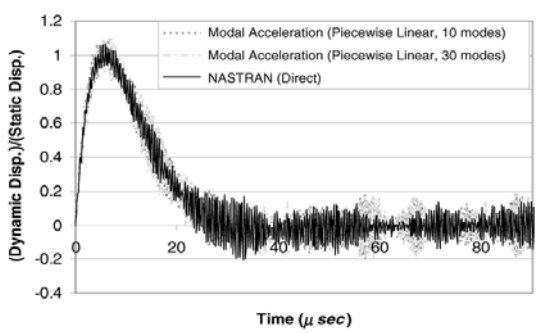

Fig. 14 Time history of the change in the length of gap obtained with the modal acceleration method and the NASTRAN direct method. The two sets of results are in good agreement

comparison of CPU time using a Sun Blade 1000 Workstation when normal mode and static displacement calculations were given. Also, the advantage of the modal acceleration method over the modal superposition method is found to be that the former requires a lesser number of modes to be extracted, thus saving time.

3. Structural optimization

The objective in this design study is to minimize the size and the weight of the sensor which can sustain a 50,000 psi pressure wave. The design constraints are that the fundamental frequency in the axial direction should be greater than 1 MHz and that the structural displacement at the gap should be less than 1 nm. Also, the design has to prevent silicon failure and prevent fiber rebound failure. The fixed values in this design are the fiber diameter (124 mm), gap length (100 mm), V-groove etch angle (54.7°), and bond length (larger than 2 mm).

Therefore the design parameters are to be the size of the silicon base (height, width, and depth (H, W, D)), the size of the rectangular shaped groove (width and depth (Wg, Dg)), the depth of the V-groove (Dv), and the exposed length of the fiber (Lf). From the design constraints, the related geometrical constraints were found to be

$$H > Dg > Dv > 169.3 \text{ mm},$$
$$|Wg - Lf| > 100 \text{ mm}$$

In performing a parametric design study on the sensor, the MATLAB code that can connect the input and output of NASTRAN to the MATLAB environment was used.

The steps followed in this parametric study are

as follows.

The first step in performing the parametric study on the design of the sensor was to obtain the response of the sensor for different dimensions of the sensor. A MATLAB code was used to automatically generate input files for NASTRAN with different dimensions of the sensor. Next, a NN was trained for the set of the dimension of the sensor and the calculated response of the sensor such that for a given dimension of the sensor, the NN can output the response of the sensor. The trained NN was tested with an unseen set of data for verification. In the next step, a gradient based optimization was performed on the input and output mapping of the trained NN. The objective was minimizing the overall volume of the sensor. The constraints were the minimum of 1 MHz natural frequency and the maximum of 1 n m displacement at the gap. The calculations of the constraints were performed quickly using the trained NN. The constrained nonlinear multivariable optimization function in the optimization toolbox of MATLAB was used to find the optimal dimensions of the sensor.

The overall step is shown as a flow chart in Fig. 15. This whole process involving NASTRAN analysis was performed automatically in the MATLAB environment.

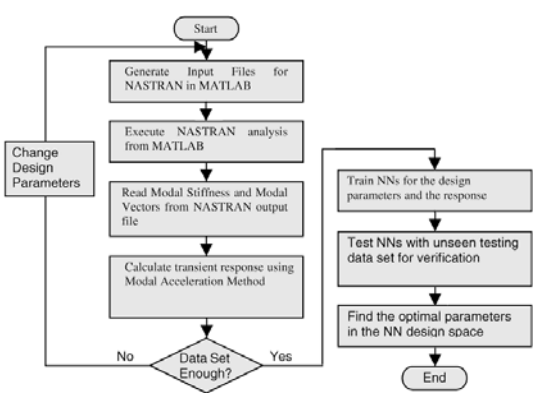

Fig. 15 The procedure in the parametric study of the design of the sensor. The ability to run NASTRAN from MATLAB without any human intervention greatly facilitated the data generation for training Neural Networks

The responses of the sensor calculated for each set of dimensions were the first natural frequency and the peak displacement at the gap when 50,000 psi peak pressure was applied at the top of the sensor in the functional form shown in Fig. 9. Multi-layer feed-forward back-propagation NNs were used with a resilient backpropagation learning scheme (Demuth et al., 2000).

First, the response of the sensor was obtained varying the width between 2.1 mm and 2.9 mm, length between 2.4 mm and 2.6 mm, and height between 0.4 mm and 1.2 mm using a step size of 0.1 mm. The design that fulfills exact constraints, which are 1 MHz natural frequency and 1 nm of displacement, was not achieved. The optimization that fulfilled some loose constraints, 1 MHz natural frequency and 100 nm displacement at the gap, resulted in the dimensions 2.82 mm (W), 2.41 mm (L), and 1.15 mm (H).

The response of the sensor was obtained for a broader range of dimensions. The width was varied between 2.5 mm and 3.5 mm, length between 2.3 mm and 3.5 mm, and height between 0.8 mm and 2.0 mm. The optimization, which fulfilled loose constraints 1 MHz frequency and a gap displacement of 100 nm, resulted in the width 2.69 mm, length 2.3 mm, and height 1.15 mm. A verification run of MATLAB and NASTRAN resulted in 1.18 MHz natural frequency and 142 nm of displacement at the gap.

4. Conclusions

A miniature fiber optic sensor was analyzed for its reliability against high peak pressure. Moreover, a parametric study was performed to obtain optimal dimensions for the sensor. The normal mode solution made sure the design of the sensor was within the limit of the natural frequency. The parametric study utilizing NASTRAN normal mode analysis for the displacement constraints and neural networks found the desired design without the need for solving possible direct problem existing in the design space.

The first step in solving inverse problems is finding the best information that will most efficiently identify the parameters that we are seeking.

The first natural frequency and the maximum deflection in transient analysis of a fiber optic sensor were the constraints in solving the problem. The second step lies in finding the best structure and training method to employ NN to solve the specific inverse problem. Multilayer Feed-Forward Backpropagation NN which has 2 hidden layers that uses sigmoid transfer functions for hidden layers and a linear transfer function for output layer and employs a resilient backpropagation training scheme was found to be most efficient.

The code developed in the MATLAB environment that can automatically connect NASTRAN solid FE analysis to MATLAB analysis made it possible to generate enough training data for NN. Moreover, this code has made it possible to use highly complex NASTRAN structural models in an analysis or a design process that involves NN and other analyses like the modal superposition method and Fast Fourier Transform analysis in the MATLAB environment.

Acknowledgments

The authors wish to thank Luna Innovations Inc., Blacksburg, VA, USA and Center for Healthcare Technology Development, Chonbuk National University, South Korea for the valuable supports.

References

Baker, W. E., 1973, *Explosions in Air*, University of Texas Press, Austin.

Cho, J. R., Jeong, H. S., Yoo, W. S. and Shin, S. W., 2004, "Optimum Tire Contour Design Using Systematic STOM and Neural Network," *KSME International Journal*, Vol. 18 No. 8, pp. 1327～1337.

Craig, R. R., 1981, *Structural Dynamics : An Introduction to Computer Methods*, Wiley, New York.

Demuth, H. and Beale, M., 2000, *Neural Network Toolbox for Use with MATLAB*, The Math Works Inc., pp. 5.16～5.17.

Greenman, R.M., Stepniewski, S.W., Jorgensen, C. C. and Roth, K. R., 2002, "Designing Compact Feedforward Neural Models with Small Training Data Sets," *Journal of Aircraft*, Vol. 39, No. 3, pp. 452～459.

Ha, I. C. and Han, M. C., 2004, "A Robust Control with a Neural Network Structure for Uncertain Robot Manipulator," *KSME International Journal*, Vol. 18 No. 11, pp. 1916～1922.

Hadi, M. N. S., 2003, "Neural Networks Applications in Concrete Structures," *Computers and Structures*, Vol. 81, pp. 373～381.

Hagan, M. T., 1996, Demuth, H. B. and Beale, M., *Neural Network Design*, PWS Publishing Company, Boston, MA.

Haykin, S. S., 1998, *Neural Networks : Fundamental Foundation, 2nd Ed*, Prentice Hall, Upper Saddle River

Kaufman, K. R., Wavering, T., Morrow, D., Davis, J. and Lieber, R. L., 2003, "Performance Characteristics of a pressure microsensor," *Journal of Biomechanics*, Vol. 36, pp. 283～287.

Kaveh, A. and Servati, H., 2001, "Design of Double layer Grids Using Backpropagation Neural Networks," *Computers and Structures*, Vol. 79, pp. 1561～1568.

Kersey, A. D., 1996, "A Review of Recent Developments in Fiber Optic Sensor Technology," *Optical Fiber Technology*, Vol. 2, pp. 291～317.

Kim, S. Y., Moon, B. Y. and Kim, D. E., 2004, "Optimum Design of Ship Design System Using Neural Network Method in Initial Design of Hull Plate," *KSME International Journal*, Vol. 18, No. 11, pp. 1923～1931.

Lee, B., 2003, "Review of the Present Status of Optical Fiber Sensors," *Optical Fiber Technology*, Vol. 9, pp. 57～79.

Lee, E. D., Sim, J. H., Kweon, H. J. and Paik, I. H., 2004, "Determination of Process Parameters in Stereolithography Using Neural Network," *KSME International Journal*, Vol. 18, No. 3, pp. 443～452.

Leung, C. K. Y., Yang, Z., Ying, X., Tong, P. and Lee, S. K. L., 2005, "Delamination Detection in Laminate Composites with an Embedded Fiber Optical Interferometric Sensor," *Sensors and Actuators A — Physical*, Vol. 119, pp. 336～344.

Li, H. N., Li, D. S. and Song, G. B., 2004,

"Recent Applications of Fiber Optic Sensors to Health Monitoring in Civil Engineering," *Engineering Structures*, Vol. 26, pp. 1647～1657.

Li, Z., Kapania, R. K. and Spillman, W. B., 2004, "Placement Optimization of Fiber Optic Sensors for a Smart Bed Using Genetic Algorithms," *Proceedings of the 10th AIAA/ISSMO Multidisciplinary Analysis and Optimization Conference*, Albany, NY.

Mukherjee, A. and Deshpande, J. M., 1995, "Application of Artificial Neural Networks in Structural Design Expert Systems," *Computers and Structures*, Vol. 54, No. 3, pp. 367～375.

Nikolaidis, E., Long, L. and Ling, Q., 2000, "Neural Networks and Response Surface Polynomials for Design of Vehicle Joints," *Computers and Structures*, Vol. 75, pp. 593～607.

Park, J. H. and Seo, K. K., 2003, "Approximate Life Cycle Assessment of Product Concepts Using Multiple Regression Analysis and Artificial Neural Networks," *KSME International Journal*, Vol. 17, No. 12, pp. 1969～1976.

Rai, M. M. and Madavan N. K., 2000, "Aerodynamic Design Using Neural Networks," *AIAA Journal*, Vol. 38, No. 1, pp. 173～182.

Ramasamy, J. V. and Rajasekaran, S., 1996, "Artificial Neural Network and Genetic Algorithm for the Design Optimization of Industrial Roofs," *Computers and Structures*, Vol. 58, No. 4, pp. 747～755.

Spillman, W. B., Mayers, M., Bennett, J., Gong, J., Meissner, K. E., Davis, B., Claus, R. O., Muelenaer Jr, A. A. and Xu, X., 2004, "A 'Smart' Bed for Non-intrusive Monitoring of Patient Physiological Factors," *Measurement Science and Technology*, Vol. 15, pp. 1614～1620.

Yang, C., Zhao, C., Wold, L. and Kaufman, K. R., 2003, "Biocompatibility of a Physiological Pressure Sensor," *Biosensors and Bioelectronics*, Vol. 19, pp. 51～58.